Numerical Simulation of Coherent Extreme Ultraviolet Radiation by Considering Simple Hydrogen Atomic Potential

Muhammed SAYRAC[1*]

Highlights:
- Keldysh parameter
- Lewenstein model
- Electron trajectories
- Dipole moment

Keywords:
- Keldysh parameter
- Lewenstein model
- Electron trajectories
- Dipole moment

ABSTRACT:

In this study, the ionization of a single electron exposed to an intense laser field is computed, and the nonlinear dipole response of a single electron is obtained. The ionization of a single electron exposed to an intense laser field can be computed using the strong field approximation (SFA), also known as the Keldysh theory. This method is based on the idea that the laser field is so strong that it can ionize the electron by tunneling through the Coulomb barrier. In this paper, the Xe, Ne, and H_2 gas species are modeled since they have simple atomic systems. All gas species have relative or close ionization potentials. Ultra-short pulse duration (50 fs) is accepted because of the shorter time scale than the electron energy-lattice transfer. The ionization potentials of gas species result in the Keldysh parameter being smaller than one. The electron dipole oscillation spectra of these gas species are simulated by calculating the dipole spectrum considering the Lewenstein model. The electron propagation under the different wavelengths is simulated. The effects of the different driving wavelengths have noticeable effects on the enhancement and the extension of the extreme ultraviolet radiation signal.

[1] Muhammed SAYRAC (Orcid ID: 0000-0003-4373-6897), Department of Nanotechnology Engineering, Sivas Cumhuriyet University, Sivas, Türkiye

*Corresponding Author: Muhammed SAYRAC, e-mail: muhammedsayrac@cumhuriyet.edu.tr

INTRODUCTION

The development of the first laser goes back to the 1960s for the generation of coherent IR radiation. The lasers work by taking into account the population of inversion in the laser medium. The radiation wavelength is usually generated at about >200 nm. The advancement in nanoscale materials requires a laser wavelength below 100 nm which corresponds to coherent X-ray radiation.

There are light sources for the generation of high-power radiation (<100 nm), i.e. synchrotrons and free-electron lasers (FELs) (Potylitsyn A.P., 2010). However, these synchrotron sources are not coherent and are generated by electrons under the spatially periodic magnetic field (Zhukovskii and Kalitenko, 2020). On the other hand, FELs have obtained coherent IR radiation from electrons separated from each other by one wavelength. This phenomenon is used in FEL to generate coherent X-ray radiation (Huang and Kim, 2007; Mcneil and Thompson, 2010; Pellegrini, 2016; Pellegrini et al., 2016). X-ray radiation finds applications in various areas from science to technology, and from medicine to architecture (Albertin et al., 2015; Hwu et al., 2017; Huang et al., 2018; G. Margaritondo, 2019). The weak efficiency of X-ray reflecting elements, and the generated radiation using FELs should be a high gain (Kroll and Mcmullin, 1978; Kim and Xie, 1993). High energy electrons are generated at a single pass. This structure and high current are needed to obtain a coherent X-ray source. Such an X-ray source setup could have a relatively big size reaching a kilometer range.

Generation of coherent X-ray radiation from high harmonic generation (HHG) setups is a promising way to obtain such radiation because the size of this source is small and economically affordable compared to the FELs (Shaftan and Yu, 2005; Deng and Dai, 2013; Li and Jia, 2013). The oscillation of the electrons, which is controlled by the electron dynamics under the intense laser field is a nonlinear phenomenon. The strong laser field affects the single-atom response. The macroscopic effects on the generation of coherent XUV pulses directly depend on the driving field features, namely central wavelength, and pulse duration to name just a few.

The laser-matter interaction results in the ionization of the medium. In 1993, Corkum et. al. explained laser-matter interaction (Corkum, 1993), tunnel ionization, acceleration, and recombination. These three-step explanations clarify the generation of coherent XUV pulses mechanism. The semi-classical model explains the electron behavior exposed to a strong driving field. The maximum obtained XUV pulse energy is determined by the cutoff energy

$$\hbar\omega_c \approx 3.17 U_p + I_p \tag{1}$$

here $u_p \sim \frac{1}{\omega_0^2}$ is called ponderomotive energy. The cutoff energy is related to the ionization potential of the used medium (I_p) and the laser field intensity (I).

Moreover, the quantum mechanical explanation for the generation of coherent XUV pulses was provided by Lewenstein et. al. (Lewenstein et al., 1994). The scope of this study is to obtain an electron excursion time by considering the Lewenstein model, and the dipole spectrum of a single atom response is obtained. The novelty of this work is to obtain the dipole spectrum of an electron for the combination of the short and long electron trajectories. Moreover, the driving laser parameters affect the dipole spectrum of the electron. The Fourier transformation of dipole response is calculated with the MATLAB program using the Lewenstein approach (Lewenstein et al., 1994). Xenon (Xe), Neon (Ne), and molecular hydrogen (H_2) gases are used as interaction mediums because they are noble gases at standard temperature and pressure.
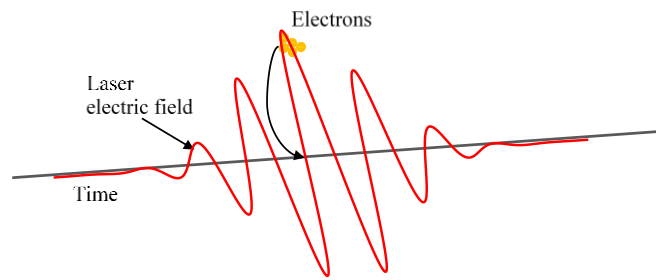
Figure 1. Electric field visualization of laser-matter interaction

MATERIALS AND METHODS

Theoretical part

The behaviors of electrons exposed to intense laser fields and wavelengths are investigated by considering the Lewenstein model using the hydrogen-like atomic model. The Gaussian pulse shape is used in the simulation. The visualization of the electron under the laser field is presented in Fig. 1.

The Lewenstein model is outlined in Ref. (Lewenstein et al., 1994). The time-dependent Schrödinger equation (TDSE) is a fundamental equation in quantum mechanics that describes how the wave function of a quantum system changes over time. It is a partial differential equation that governs the evolution of the wave function, which encodes all of the information about the system, including its position, momentum, energy, and other physical properties. The TDSE for one electron system is written as

$$i\frac{\partial}{\partial t}|\psi(t)\rangle = \left[-\frac{1}{2}\nabla^2 + V(r) - ECos(t)x\right]|\psi(t)\rangle \tag{2}$$

here the atomic potential is $V(r)$, and additional potential $ECos(t)x$ is due to the driving laser. The TDSE has been solved by considering three assumptions (Lewenstein et al., 1994): (i) the only bound state plays a role in the evolution of the system, (ii) the depletion of the ground state is neglected, and (iii) there is no overlap of the continuum states with the ground state.

To compute the dipole spectrum of the electron, one needs to solve the time-dependent Schrödinger equation (TDSE) for the electron in the presence of the laser field. The solution to the TDSE can be written in terms of the eigenstates of the TDSE in the presence of the laser field.

There are several approaches to solving the TDSE, including the semiclassical approximation and numerical methods such as the split-operator method. In general, the accuracy of the solutions depends on the intensity of the laser field and the duration of the pulse. At very high intensities or very short pulse durations, other effects such as multiphoton ionization and rescattering may become important and must be taken into account. In this presented simulation, moderate laser intensities on the order of 10^{14}W/cm^2 are used as the input parameters.

By considering the TDSE, the dipole moment of the electron is obtained from the electron trajectories. The dipole moment is given (Lewenstein et al., 1994)

$$d(t) = -er(t) = -\langle\psi(t)|\hat{r}|\psi(t)\rangle \tag{3}$$

and

$$d(t) = -ie_x\int_0^\infty d\tau\left(\frac{\pi}{\varepsilon + i\tau/2}\right)^{3/2}.E\cos(t-\tau).D_x(p_s(t,\tau) - A_x(t-\tau)) \times \exp(-iS_s(t,\tau)).D_x^*(p_s(t,\tau) - A_x(t)) + c.c. \tag{4}$$

where $E\cos(t-\tau).D_x(p_s(t,\tau)-A_x(t-\tau))$ is the probability amplitude that the driving field $E\cos(t-\tau)$ releases the electron to the continuum. $D_x(p_s(t,\tau)-A_x(t-\tau))$ gives a coupling of the ground state to the vacuum continuum state. The second term $\exp(-iS_s(t,\tau))$ is the phase that the electron acquires during propagation, and S_s is the quasi-classical action corresponding to the electron trajectory.

The third term $D_x^*(p_s(t,\tau)-A_x(t))$ gives probability amplitude for recombination, which is due to the interference of the ground state wave function with the returning wave packet. The distribution of the dipole spectra was obtained by solving the TDSE (Lewenstein et al., 1994).

On the other hand, there are restrictions while solving the TDSE. The magnetic field is ignored for the laser intensities lower than 10^{16} W/cm^2. Moreover, the driving laser wavelength ($\lambda<2000$ nm) is accepted (Bhardwaj, 2010). With these assumptions, the electron freely propagates under the laser field without the effect of the Coulomb potential. This phenomenon occurs when the electron kinetic energy is high (high driving field intensity). The Keldysh parameter (Keldysh, 1965) defines the laser intensity as high enough for tunneling ionization

$$\gamma \approx \sqrt{\frac{I_p}{2U_p}} \tag{5}$$

If the Keldysh parameter is smaller than the one $(\gamma<1)$, it means to tunnel ionization. When $\gamma>1$ it indicates the multi-photon channels in the transition regime (Hao et al., 2016).

High driving field intensity causes the target atoms partially ionized over one driving field. The dipole response of the electron is affected due to the depletion of the ground state. In these theoretical approaches, zero ground state depletion is considered as referenced in the Lewenstein model (Lewenstein et al., 1994).

Dipole response calculates the oscillating of an electron at the frequency of the driving laser field. Driving laser parameters (Intensity, wavelength, etc.) determine the distribution of the dipole response. The high laser intensities, the electron oscillates at high laser frequencies, which results in nonlinear phenomena. This nonlinear response leads to the generation of high-energy photons. The MATLAB program is used to calculate the dipole spectrum of the electrons under the intense laser field. The distribution of high-energy photons is obtained at different driving laser fields.

RESULTS AND DISCUSSION

Simulation of dipole spectra for different atoms and driving field wavelength is computed assuming Gaussian pulse shape. The pulse durations are set to 50 fs, and the intensity of the driving field is ~10^{14} W/cm^2. The driving field wavelengths are 800 nm and 1000 nm. The electron propagation under the laser field follows mainly short and long electron trajectories. The path of these trajectories directly affects the dipole response of an electron. The focus of this paper is to consider the contribution of both short and long-electron trajectories. The Keldysh parameter is smaller than one (<1), which justifies the tunnel ionization regime. The nonlinear dipole response of an electron is provided by taking into account the Lewenstein model. The different atom mediums produce different dipole responses due to having different ionization potentials.

These different atoms are chosen because of their different ionization potential. In addition, they are simple atomic systems. Xenon (Xe), Neon (Ne), and hydrogen molecule (H$_2$) are chosen. The ionization potentials of these gases are 12.13 eV for Xe (Technology, 2022), 21.5 eV for Ne (Womer, 1931), and 13.59 eV for H$_2$ (Bleakney, 1932).

Figure 2 exhibits the electric field of the Gaussian pulse as a function of pulse duration (fs). The full width at half-maximum pulse duration is set to 50 fs. The driving field for different wavelengths at the intensity of 10^{14} W/cm^2 is used to excite the nonlinear atomic medium. The electric field of a Gaussian pulse depends on the pulse width. In general pulse width decreases the electric field of the pulse also decreases since the electric field is proportional to the rate of change of the electric potential, i.e. shorter pulse has a small rate of change. The electric field of driven laser fields has a critical role in the harmonic generation process since it affects the ionization and acceleration of the electrons. The shape and strength of the laser field significantly affect the harmonic spectrum. A stronger electric field usually results in a higher yield of high-energy harmonics. For this reason, the pulse duration of 50fs and high laser intensity is used in the simulation to produce an optimum high harmonic generation spectral distribution.
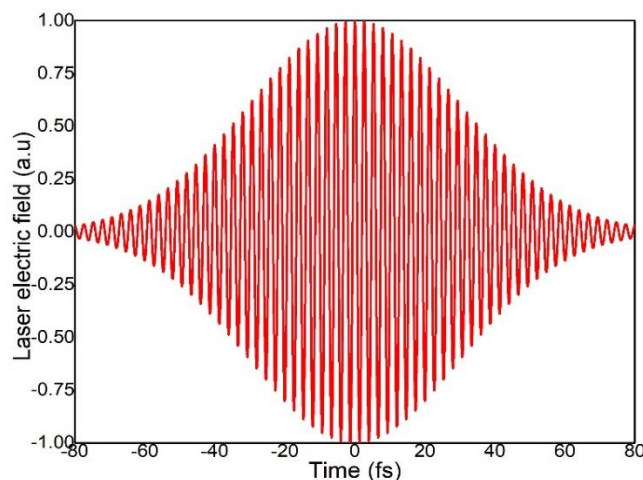
Figure 2. Electric field distribution of Gaussian pulse over pulse duration. The fundamental wavelength is 800 nm with 50 fs FWHM and an intensity of 10^{14} W/ cm^2
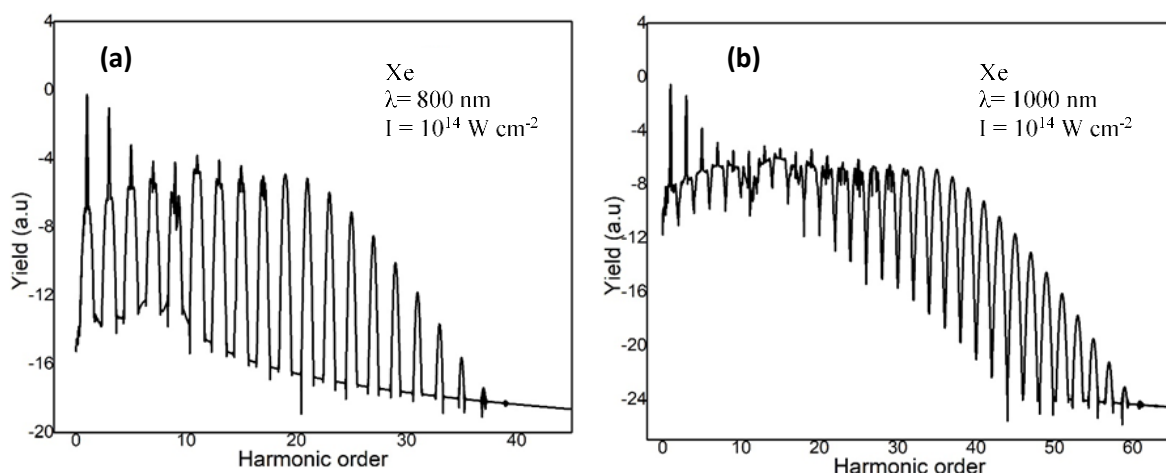
Figure 3. Electron dipole oscillation for Xe gas at different driving wavelengths (a) 800nm (b) 1000nm

Figure 3 presents the dipole spectrum for the Xe atom for a combination of short and long electron trajectories. Electron propagates under the strong-laser field at different trajectories. In theory, electron recombination mostly emits more signals at the short trajectory than the long trajectories because the electron is less exposed to the ultrashort driving field at the short trajectories. In addition, the combination of short and long trajectories causes the shift of the electrons from the propagation direction and ends up with a low signal under the short laser pulse. Figure 3 (a) demonstrates electron oscillation for the driving laser field of 800 nm while Figure 3 (b) is for the driving field of 1000 nm.

The electron propagation under the laser field and gained kinetic energy are proportional to the second power of the driving laser field ($U \sim \lambda^2$). The longer driving laser wavelength produces a strong dipole spectrum yield than the other one. This allows for more signals compared to the EUV spectrum produced at 800 nm. In addition, the electron dipole spectra extend towards higher photon energies for considering the short electron trajectories. ($\left(\frac{1240}{\lambda_{driving}}\right) \times HO$, $\lambda_{driving}$: driving laser wavelength, and *HO*: harmonic order).
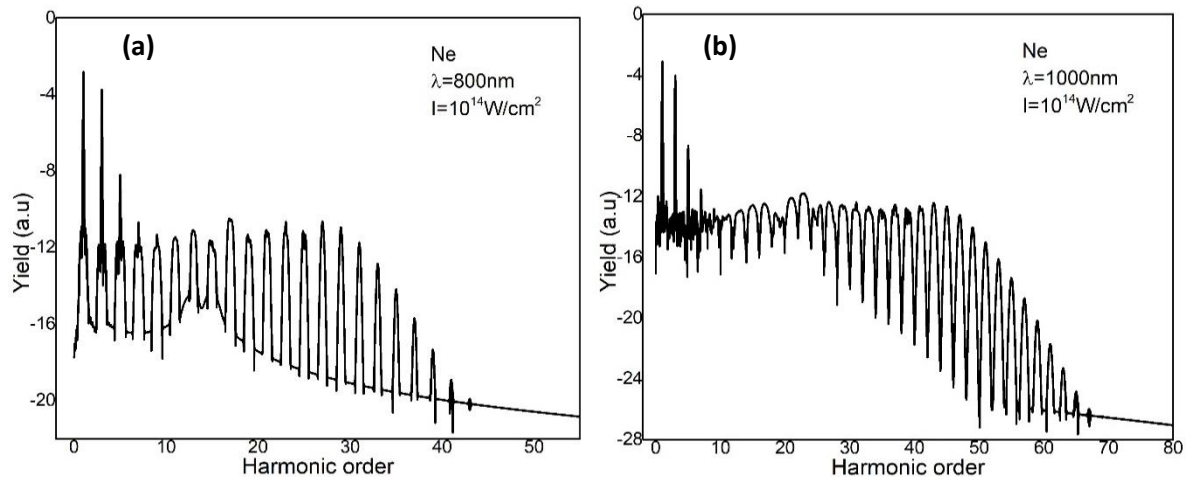
Figure 4. Electron dipole oscillation for Ne gas at different driving wavelengths (a) 800nm (b) 1000nm

Figure 4 is the simulation of the dipole oscillation of the Ne atom. The dipole spectrum extends to higher photon energies similar to the Xe atom at the longer driving wavelength. The electron dipole oscillation reaches high photon energy for the Ne atom due to its high-ionization potential. Figures 4 (b) gives more signals compared to Figure 4 (a) due to driving laser wavelength, in which electrons gained higher kinetic energy due to laser oscillation (the interference of the ionized electron wave function with the ground state wave function).
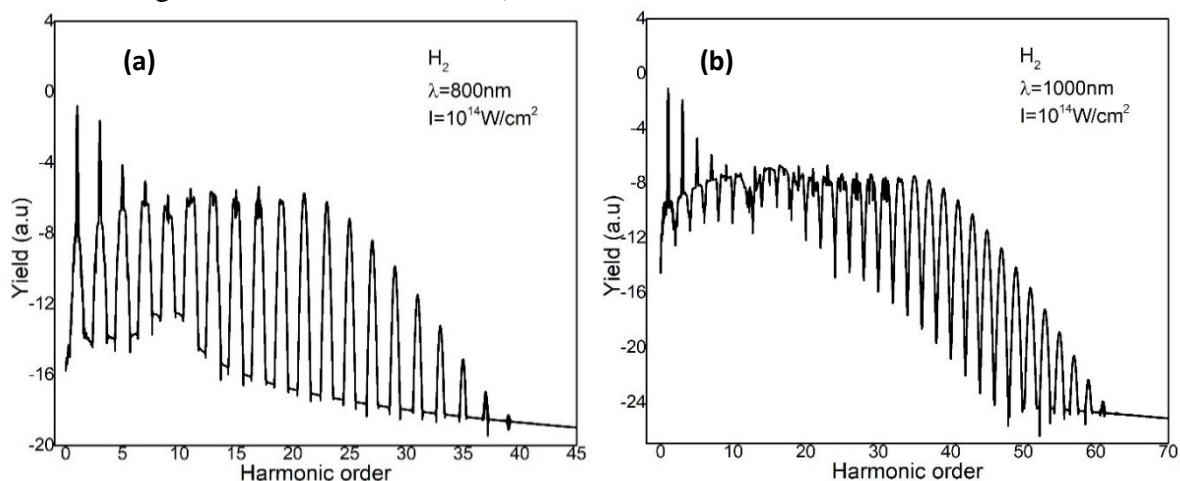
Figure 5. Electron dipole oscillation for H₂ gas at different driving wavelengths (a) 800nm (b) 1000nm

Figure 5 exhibits electron oscillation at two different driving laser wavelengths for the H$_2$ gas. The H$_2$ is the smallest molecule and diffuses the most in materials than others. For this reason, the simulation of the H$_2$ molecule is performed to understand its behavior under the short laser pulse. Figure 5 (a) is obtained for 800 nm driving field while Figure 5 (b) is for 1000 nm driving laser wavelength. The higher laser wavelength produces higher EUV pulses reaching the 60th harmonic order.
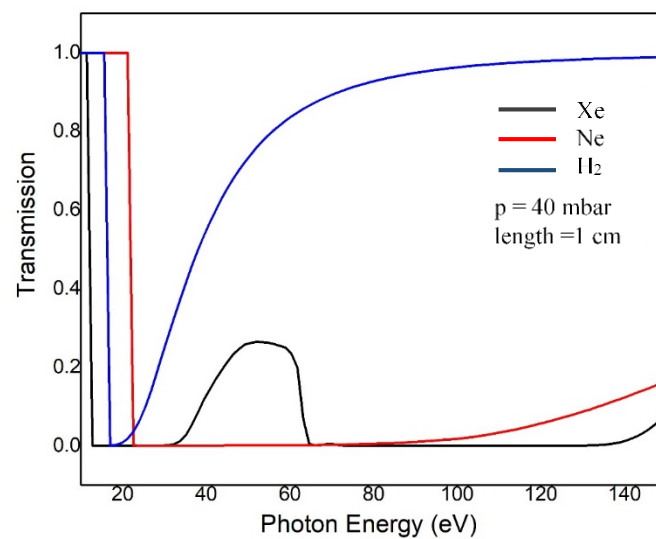
Figure 6. Transmission of Xe, Ne, and H₂ gas species at 40 mbar interaction region pressure with a 1 cm path

The transmission of the gas species through a medium is related to the change in the index of refraction of the medium. The refraction index is a measurement of how much the light wave is slowed down as it travels through the medium. The higher the refractive index, the more the light is slowed down. Transmission of the gas species through the medium is affected by the density of gas and the wavelength of the light. The gas density determines how much of the gas is present in the medium. The wavelength of the light determines how much the light is absorbed or scattered by the gas, which also affects the transmission of the light. In general, the transmission of a neutral gas species through a medium is higher when the density of the gas is lower and the wavelength of the light is longer. This is because lower gas densities and longer wavelengths result in less absorption and scattering of the light by the gas, leading to higher transmission of the light through the medium. Figure 6 presents the transmission of Xe, Ne, and H₂ gas species. The X-ray transmission of these gas species at 40 mbar through 1cm length is obtained on the Henke NIST website (Technology, 2022). Transmission of this neutral gas species is related to the change in the index of refraction, $(n=n_0+\Delta n(t))$.

CONCLUSION

In conclusion, the atomic gas species of Xe, Ne, and H₂ exposed to the strong-laser fields are theoretically studied. The numerical simulation is obtained for a simple hydrogen atom model. The time-dependent Schrödinger equation for one electron system is considered, and the dipole response for an electron exposed to a short laser field is obtained by solving the Lewenstein model. The tunnel ionization regime is justified by the Keldysh parameter $(\gamma < 1)$. For the simulation input parameters, the short and long electron trajectories are taken into account, and the different driving laser wavelengths are used. The longer driving laser field produces a strong dipole spectrum than the short laser wavelength. This study shows that the ionization rate of an electron is mainly affected by ionization potential and the external driving laser field. As a result, emitted photon energy increases upon recombination. Absorption of the used gas species is plotted from the Henke webpage. The absorption of the gas species on the EUV pulse amplitude restricts the coherent buildup of the emitted radiation. The numerical simulation helps pre-experimental studies in estimating the necessary parameters to understand how laser-matter interaction plays a role in the generation of coherent optical pulses. By using computational models to simulate the laser-matter interaction, the physical

mechanism is better understood and the performance of the harmonic signal is optimized as well as the predict the expected outcome of an experiment.

Conflict of Interest

The author declared that there is no conflict of interest.

REFERENCES

Albertin F, Astolfo A, Stampanoni M, Peccenini E, Hwu Y, Kaplan Fr, Margaritondo G, (2015). X-Ray Spectrometry and Imaging for Ancient Administrative Handwritten Documents. X-Ray Spectrometry, 44:93-98.

Bhardwaj S, (2010). Limits of Long Wavelength High Harmonic Generation. Department of Electrical Engineering. Massachusetts Institute of Technology, Massachusetts Institute of Technology. Doctorate.

Bleakney W, (1932). The Ionization Potential of Molecular Hydrogen. Physical Review Letters, 40:496-501.

Corkum PB, (1993). Plasma Perspective on Strong-Field Multiphoton Ionization. Physical Review Letters, 71:1994-1997.

Deng H-X, Dai Z-M, (2013). Harmonic Lasing of X-Ray Free Electron Laser: On the Way to Smaller and Cheaper. Chinese Physics C, 37:102001.

Hao X, Shu Z, Li W, Hu S, Chen J, (2016). Quantitative Identification of Different Strong-Field Ionization Channels in the Transition Regime. Optics Express, 24:25250-25257.

Huang C-F, Liang KS, Hsu T-L, Lee T-T, Chen Y-Y, Yang S-M, Chen H-H, Huang S-H, Chang W-H, Lee T-K, Chen P, Peng K-E, Chen C-C, Shi C-Z, Hu Y-F, Margaritondo G, Ishikawa T, Wong C-H, Hwu Y, (2018). Free-Electron-Laser Coherent Diffraction Images of Individual Drug-Carrying Liposome Particles in Solution. Nanoscale, 10:2820-2824.

Huang Z, Kim K-J, (2017). Review of X-Ray Free-Electron Laser Theory. Physical Review Special Topics - Accelerators and Beams, 10:034801.

Hwu Y, Margaritondo G, Chiang A-S, (2017). Q&A: Why Use Synchrotron X-Ray Tomography for Multi-Scale Connectome Mapping? BMC Biology, 15:122.

Keldysh LV, (1965). Ionization in the Field of a Strong Electromagnetic Wave. Sov. Phys.-JETP, 20.

Kim K-J, Xie M., (1993). Self-Amplified Spontaneous Emission for Short Wavelength Coherent Radiation. Nuclear Instruments and Methods in Physics Research Section A: Accelerators, Spectrometers, Detectors and Associated Equipment, 331:359-364.

Kroll NM, McMullin WA, (1978). Stimulated Emission from Relativistic Electrons Passing through a Spatially Periodic Transverse Magnetic Field. Physical Review A, 17:300-308.

Lewenstein M, Balcou P, Ivanov MY, L'Huillier A, Corkum PB, (1994). Theory of High-Harmonic Generation by Low-Frequency Laser Fields. Phys. Rev. A, 49:2117-2132.

Li H-T, Jia Q-K, (2013). Enhanced High Gain Harmonic Generation Scheme with Negative Dispersion. Chinese Physics C, 37:028102.

Margaritondo G, (2019). An Enlightening Procedure to Explain the Extreme Power of Synchrotron Radiation. J. Synchrotron Rad., 26:2094-2096.

McNeil BWJ, Thompson NR, (2010). X-Ray Free-Electron Lasers. Nature Photonics, 4:814-821.

Pellegrini C, (2016). X-Ray Free-Electron Lasers: From Dreams to Reality. Physica Scripta, T169, 014004.

Pellegrini C, Marinelli A, Reiche S, (2016). The Physics of X-Ray Free-Electron Lasers. Reviews of Modern Physics, 88:015006.

Potylitsyn A.P. RMI, Strikhanov M.N., Tishchenko A.A. (2010). Radiation from Relativistic Particles. In: Diffraction Radiation from Relativistic Particles. Springer Tracts in Modern Physics, , Springer, Berlin, Heidelberg.

Shaftan T, Yu LH, (2005). High-Gain Harmonic Generation Free-Electron Laser with Variable Wavelength. Physical Review E, 71:046501.

Technology NIoSa (2022). "Nist Chemistry Webbook." 2021, from https://webbook.nist.gov/.

Womer R, (1931). Ionization of Helium, Neon, and Argon. Physical Review, 38, 454-456.

Zhukovskii KV, Kalitenko AM, (2020). Generation of Coherent X-Ray Harmonic Radiation in a Single-Pass Free-Electron Laser with Phase Shift of Electrons Relative to Photons. Technical Physics, 65:1285-1295.